



On the Development of a Nomogram for Alkali Activated Fly Ash Material (AAFAM) Mixtures

Partogi H. Simatupang¹, Iswandi Imran², Ivindra Pane² & Bambang Sunendar³

¹Faculty of Science and Engineering, University of Nusa Cendana,
Jalan Adisucipto-Penfui, Kota Kupang, Indonesia

²Department of Civil Engineering, Bandung Institute of Technology,
Jalan Ganesha 10, Bandung 40132, Indonesia

³Department of Physics Engineering, Bandung Institute of Technology,
Jalan Ganesha 10, Bandung 40132, Indonesia
Email: simatupangpartogi@yahoo.com

Abstract. Alkali activated fly ash material (AAFAM) has become the most promising material to substitute materials based on ordinary Portland cement (OPC). However, there is no available nomogram for AAFAM mixtures. In contrast, there are many rational methods available in the literature to make paste, mortar and concrete with OPC based materials, such as Monteiro-Helene's nomogram, which uses Abram's law, Lyse's law and Molinari's law. This paper presents a study to construct such a nomogram for AAFAM mixtures by first conducting experiments on the paste and mortar phases. The procedure of Monteiro-Helene's nomogram was adopted in this formulation. The first step in this direction was to find a close relationship between the strength and paste composition of the material that can be used as a substitute for Abram's law. The second step was to construct the equivalent of Lyse's and Molinari's relationships by varying the sand and fly ash contents. The results show that it is possible to make a nomogram for AAFAM mixtures such as the one for OPC based materials. Class F fly ash and its mortar phase were used to construct the nomogram. In addition, the mortar samples that were used to build the nomogram had similar solidification products according to their microscopic characteristics.

Keywords: *alkali activated fly ash material; Monteiro-Helene's nomogram; mortar phase; nomogram; paste phase*

1 Introduction

Alkali activated material (AAM) is a solid material formed by alkali activation on silica and alumina-rich materials. Hence, AAM basically does not need ordinary Portland cement (OPC) as a binder. This is actually not a new technology. Davidovits [1] and Pachecho-Torgal, *et al.* [2] have traced back the history of this material and its application to the 1950s. Duxson, *et al.* [3] list different names for it, i.e. low-temperature aluminosilicate glass, alkali-activated cement, geocement, alkali-bonded ceramic, inorganic concrete and

hydroceramic. However, Davidovits in 1979 named it geopolymer, which is the generic name for alkali activated material with amorphous to semicrystalline reaction products [1].

Fly ash based alkali activated material, or alkali activated fly ash material (AAFAM), has become the most promising material to substitute OPC-based materials because of its strength, durability and environmental aspects [2,3]. Pacheco-Torgal, *et al.* [2] and Duxson, *et al.* [3] have collected many researches about AAFAM and concluded that it is not difficult to produce this type of material with high strength characteristics (> 50 MPa), especially with dry curing. It is even reported that AAFAM paste can achieve remarkable strength: 90-95 MPa after 28 days [1]. In addition, durability and environmental aspects of AAFAM are also found better than those of conventional OPC binders. Fernandez-Jimenez *et al.* [4] reported that AAFAM paste and mortar are more durable than those of OPC in a sulphate and seawater environment. Its capacity can be increased by using the calcination of fly ash at 600°C [5]. This fact is basically a consequence of the absence of the mineral $\text{Ca}(\text{OH})_2$ in AAFAM solidification products [6]. As for the environmental aspect, to make one ton of AAFAM requires low energy and emits only ± 0.184 ton of CO_2 [1]. This figure is much lower when compared with OPC production, which emits approximately one ton of CO_2 for every ton of clinker.

Apart from all these benefits of AAFAM, field application of AAFAM is still very limited [7]. According to the report by Van Deventer *et al.* [7], the volume of AAFAM that has been applied recently in construction fields in Australia is small. However, application of this material on a large industrial scale is still not feasible yet. No standards, guidelines or corresponding nomogram are available to support the application of this material in the field. Thus, a standard framework for designing AAFAM should be developed [7]. The development of a nomogram for AAFAM mixtures is one important step in fulfilling that standard framework. This paper presents the development of a nomogram for AAFAM mixtures. The procedure of Monteiro-Helene's nomogram was adopted in this development.

2 Method on Material Mixtures

Methods of mix-proportioning of OPC based materials have been developed since 1828. This period can be divided into five periods: (1) First Period (1828-1891), beginning of the technology of cements, mortars and concretes; (2) Second Period (1892-1951), classical methods of mix proportioning; (3) Third Period (1936-1978), statistical methods; (4) Fourth Period (1950-1978) comprehensive models, and (5) Fifth Period (1958-1993), improvement of methods [8].

In 1994, Monteiro and Helene [8] have proposed a nomogram for quick prediction of the fresh and hardened properties of OPC based concrete. They used three basic relationships well-known in OPC material practice, i.e. Abram's law, Lyse's law and Molinari's law. The concept of Monteiro-Helene's nomogram is given in Figure 1. Abram's law describes the relationships between water/cement (w/c) and compressive strength of concrete. Lyse's law describes the relationships between water/cement (w/c) and aggregate/cement ratio for various consistencies of concrete. This means that when using the same materials, it is possible to get concrete mixtures of equal consistency by keeping the ratio between volume of water to volume of compacted fresh concrete constant [8]. Molinari's law describes the relationship between cement content and aggregate/cement ratio.

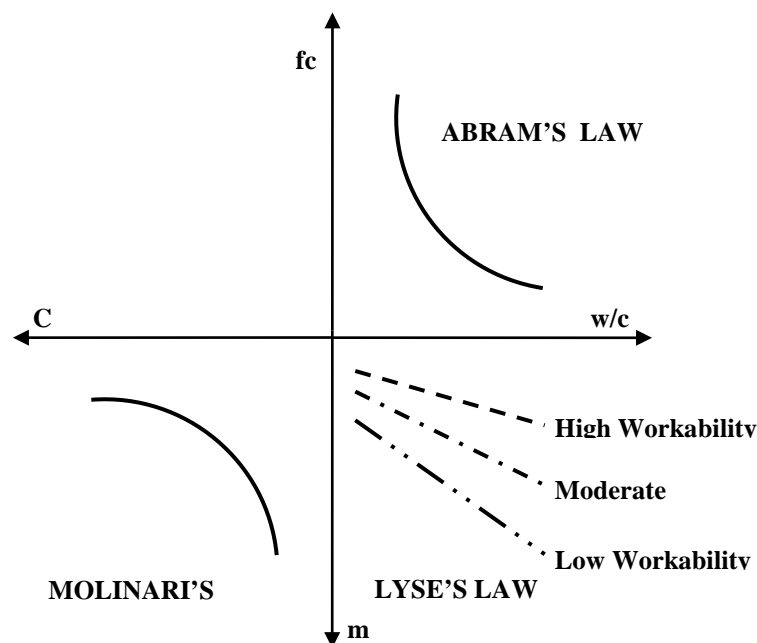


Figure 1 The concept of Monteiro-Helene's nomogram.

Up to now, there is no such nomogram for AAFAM mixtures. Nevertheless, many researchers have conducted significant steps towards constructing one. Hardjito and Rangan [9], from the Geopolymer Concrete Research Group of Curtin University of Technology Australia, have conducted a massive research on the concrete phase of AAFAM to identify the effect of salient parameters for manufacturing and developing the mixture proportioning of the material. As in the conclusions of their report, there are two paste composition factors that significantly affect the compressive strength of the material: (1) ratio of molar

reactant $\text{H}_2\text{O}/\text{Na}_2\text{O}$ (if this molar ratio increases, the compressive strength decreases), and (2) ratio of mass of water/geopolymer solids (if this ratio increases, the compressive strength decreases). They recommended these factors as mixture design parameters. However, no further information is stated about which one of these parameters is the most significant for substituting water/cement (w/c) as in OPC based material.

Based on the works of Hardjito and Rangan [9] described earlier, Anuradha, *et al.* [10] have recently presented guidelines for geopolymer concrete mix design modifying the Indian standard on OPC based concrete on a trial-and-error method. Unfortunately, there are many boundaries implied in these guidelines, such as: (1) the range of compressive strength considered is very narrow, i.e. 20-30 MPa; (2) a constant concentration of sodium hydroxide is used; and (3) qualitative information about the consistency of material is lacking. Furthermore, there is no information about the paste composition factor that can be used to substitute water/cement (w/c) as in OPC based material practices.

3 Experimental Details

3.1 Materials

The fly ash used to make AAFAM in this research was Class F fly ash from the Suralaya Coal Fired Power Plant in Banten, Indonesia. The oxides of this fly ash, analyzed using an Advant'XP+ ThermoARL XRF spectrometer, were: SiO_2 52.30%, Al_2O_3 26.57%, Fe_2O_3 7.28%, CaO 6.00%, Na_2O 1.41%, SO_3 0.70%, K_2O 0.73%, MgO 2.13% and LOI 1.18%. According to the Gravimetry test taken, the fly ash consisted of 51.20% total SiO_2 , 41.70% reactive SiO_2 and 9.53% free SiO_2 . The shape of the fly ash was spherical, based on SEM images using a JEOL JSM 6360LA. By using a Fritsch particle size analyzer (PSA) it was found that almost 50% of the fly ash grains had a diameter lower than 6 μm .

Local sand, i.e. Galunggung sand in saturated surface dry (SSD) condition, was used as fine aggregate for making the mortar phase. Its gradation complied with Gradation No. 1 (coarser sand) according to the Indonesian Standard (SNI 03-2834-1993). Bulk specific gravity (in SSD) is 2.31. The alkali activator solution used was sodium silicate solution and sodium hydroxide solution. Sodium hydroxide solution was made by dissolving NaOH flakes in aquades. NaOH flakes were at 98% purity. The sodium silicate solution was composed of SiO_2 37.23% and Na_2O 15.98% with specific gravity 1.6539 g/cm^3 . All chemicals were supplied by PT. Bratachem Bandung. A sodium hydroxide solution was added to the sodium silicate solution at normal temperature (23-27°C). It took an elapsed time of at least 4 h after the NaOH flakes were dissolved by the

aquades. The alkali activator solution mixed in to make the alkali activated fly ash material was sodium silicate solution added with sodium hydroxide solution, which was left at least 6 h up to the moment before crystallization of sodium carbonate occurred [11]. Crystallization of sodium carbonate in the alkaline solution must be avoided, because it can reduce the workability of the mixture. The compressive strength of the paste ranges from 20-40% [12]. Pacheco-Torgal, *et al.* [13] call the crystallization of sodium carbonate a 'disadvantageous efflorescence phenomena'.

3.2 Experimental Program

Samples of the paste were in the shape of cylinders with a diameter of 27.5 mm and a height of 55.0 mm. The mixtures of the pastes were varied according to: (1) molarity of sodium hydroxide (8M, 12M and 16M); and (2) mass ratio of sodium silicate solution to sodium hydroxide solution (0.5, 1.0 and 2.0). The mass ratio of fly ash to alkaline liquid was kept constant at 2.0. No added water was given in the mixtures. There were 12 mixtures of paste phase made in this research. The mixtures of the paste phase are given in Table 1.

Table 1 Mixtures of AAFAM Paste

No	[NaOH]	Fly Ash (g)	Sodium Silicate (g)	Sodium Hydroxide (g)
P-1	8	517.19	129.30	129.30
P-2	8	517.19	172.40	86.20
P-3	8	517.19	86.20	172.40
P-4	12	517.19	129.30	129.30
P-5	12	517.19	172.40	86.20
P-6	12	517.19	86.20	172.40
P-7	14	517.19	129.30	129.30
P-8	14	517.19	172.40	86.20
P-9	14	517.19	86.20	172.40
P-10	16	517.19	129.30	129.30
P-11	16	517.19	172.40	86.20
P-12	16	517.19	86.20	172.40

Meanwhile, the samples of the mortar phase were in the shape of cubes with a size of 50 x 50 x 50 mm. The mixtures of the mortars were varied according to: (1) molarity of sodium hydroxide (8M, 12M and 16M); (2) mass ratio of sodium silicate solution to sodium hydroxide solution (1.0 and 2.0); (3) mass ratio of sand to fly ash (1.80, 1.50 and 1.20), and (4) mass ratio of added water to mortar mixture (0.0%, 0.9%, 1.0%, 2.0%, 3.0% and 3.3%). The mass ratio of fly ash to alkaline liquid was also kept constant at 2.0. There were 24 mixtures of mortar phase made in this research. The mixtures of the mortar phase are given in Table 2.

Table 2 Mixtures of AAFAM Mortar.

No	[NaOH]	Fly Ash (g)	Sodium Silicate (g)	Natrium Hydroxide (g)	Sand in SSD (g)	Added Water (g)
M-1	12	1260	315	315	2268	0
M-2	8	1260	420	210	2268	0
M-3	16	1260	420	210	1890	0
M-4	8	1260	315	315	1890	0
M-5	8	1260	420	210	1890	0
M-6	12	1260	420	210	1512	0
M-7	12	1260	420	210	2268	37.8
M-8	12	1260	420	210	1890	37.8
M-9	8	1260	420	210	1890	37.8
M-10	12	1260	315	315	1890	0
M-11	16	1260	315	315	1890	37.8
M-12	16	1260	420	210	1890	75.6
M-13	12	1260	315	315	1890	37.8
M-14	12	1260	420	210	1890	75.6
M-15	16	1260	315	315	1890	0
M-16	8	1260	315	315	1890	37.8
M-17	12	1260	315	315	1512	0
M-18	8	1260	315	315	1512	0
M-19	8	1260	420	210	1890	113.4
M-20	12	1260	420	210	1890	113.4
M-21	8	1260	315	315	1890	75.6
M-22	16	1260	315	315	1890	75.6
M-23	8	1260	420	210	1890	75.6
M-24	8	1260	315	315	1890	126

3.3 Preparation, Casting and Curing of Test Specimens

The paste phase was made under ambient curing. The steps of making the geopolymer paste were as follows: pour the fly ash in a Hobart mixer pan; then pour alkali activator solution until most of the fly ash is mixed; run the Hobart mixer with a speed of 140 rpm for 30 sec; stop the Hobart mixer for a while (maximum 15 sec) to clean the side of pan; continue running the mixer at speed 280 rpm for 60 sec; run the mixer at 140 rpm for 15 sec. After the paste mixture is ready, the paste is filled into a mould in 2 (two) layers. Each layer is vibrated on the vibrating table for 30 sec. The paste mould was made by Hard Nylon. It consisted of 9 (nine) cylindrical molds of Φ 27.5 x 55.0 mm. Before use, the paste moulds were coated using vaseline. Each variable had three samples. After the paste was poured in the mould unit, the paste was left at ambient temperature for 24 h. Then, the samples were kept in clipped plastic bags until testing.

The mortar phase was made under dry curing. The steps of making the geopolymer mortar were as follows: pour sand in the Hobart mixer pan; then

pour the fly ash and mix by hand; run the Hobart mixer at 140 rpm for 3 min; pour the alkali activator solution into the dry mixture slowly; run the Hobart mixer at 140 rpm for 30 sec; stop the Hobart mixer for a while (maximum 15 sec) to clean the side of the pan; continue running the mixer at 280 rpm for 60 sec and run the mixer at 140 rpm for 15 sec. After the mortar mixture was ready, it was poured into the mortar mould in 2 (two) layers. Each layer was vibrated on the vibrating table for 60 sec. Before use, the mortar moulds were coated using vaseline. The mortar mould conformed to ASTM C 109-92. For dry curing, after the fresh mortar was poured in the mortar mould, the mould was wrapped in plastic sheets and put into an oven, which was heated up to 80 °C for 24 h. Subsequently, after the samples had attained normal temperature they were kept in clipped plastic bags until testing.

3.4 Testing of Specimens

The hardened paste and mortar were tested using a universal testing machine (UTM). The compressive strength of the paste samples at the ages of 7 and 28 days was recorded. Meanwhile, for the mortar samples, the compressive strength at the age of 7 days was recorded. This period was adopted from the research conducted by Simatupang, *et al.* [11]. They state that in dry curing, the compressive strength at the age of 7 days is almost the same as the compressive strength at the age of 28 days. Therefore, in dry curing the characteristic compressive strength of the sample is reached after 7 days. The reported compressive strength is the average strength of three specimens. The compressive testing results of the paste and mortar samples are given in Figures 2 and 3. Samples were also taken to be analyzed for microscopic characteristics using a JEOL JSM 6360LA scanning electron microscope for SEM-EDXA, a Philips Diffractometer PW 1710 XRD for an X-ray diffraction test and an FTIR Prestige 21 Shimadzu for FTIR spectrophotometry.

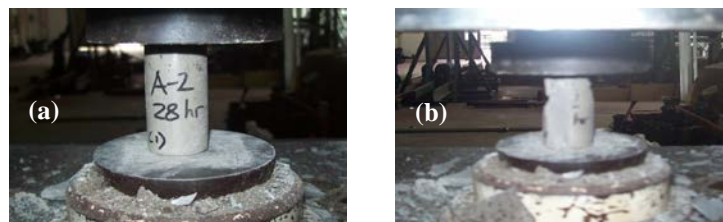


Figure 2 Compressive Testing on AAFAM paste: (a) before and (b) after.

The consistency was tested using the flow test table according to ASTM C 230-90. Before starting the test, the table and cone for the flow test were coated with vaseline to reduce the cohesive behavior between the fresh mixtures and the

metal surfaces. The ruler of the flow test table was used to measure the final diameter of the mortar after testing. The reported values are the mean of two measures of the diameter in orthogonal directions. The consistency test is shown in Figure 4.

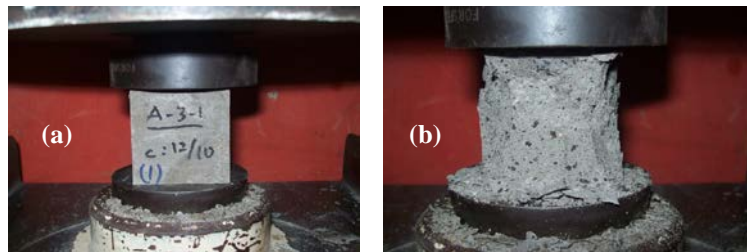


Figure 3 Compressive Testing on AAFAM Mortar: (a) before and (b) after.



Figure 4 Consistency Test of AAFAM Mortar using Flow Test Table

4 Results and Discussion

4.1 Recommendation of paste composition factor

To calculate the molar and mass ratios for the paste composition factors, the method described by Hardjito and Rangan [9], especially in Appendix B of their report, was used. This subsection presents which paste composition factor has the most significant relationship with compressive strength. The results for the AAFAM paste are given in Table 3. As shown, 5 (five) factors in paste composition were used to be correlated with compressive strength: (1) molar ratio of $\text{Na}_2\text{O}/\text{SiO}_2$; (2) molar ratio of $\text{SiO}_2/\text{Al}_2\text{O}_3$; (3) molar ratio of $\text{H}_2\text{O}/\text{Na}_2\text{O}$; (4) molar ratio of $\text{H}_2\text{O}/(\text{Na}_2\text{O}+\text{SiO}_2+\text{Al}_2\text{O}_3)$ or molar ratio of H/NSA ; and (5) mass ratio of $\text{H}_2\text{O}/(\text{Na}_2\text{O}+\text{SiO}_2+\text{Al}_2\text{O}_3)$ or mass ratio of H/NSA .

From the relationships displayed in Table 3, it can be seen that the best relationship between compressive strength and paste composition is the relationship of f_c versus molar ratio of $\text{H}_2\text{O}/(\text{Na}_2\text{O}+\text{SiO}_2+\text{Al}_2\text{O}_3)$. This relationship is presented in Figure 5. The power function of regression is the best choice with $R^2 = 0.86$ for 28 days and $R^2 = 0.93$ for 7 days. Therefore, the

relationship of f_c versus molar ratio of H/NSA in AAFAM based material was considered as a substitute for the relationship of f_c versus w/c in OPC based material. Below, this relationship will be verified by secondary data. The next subsection presents the application of the relationship on higher phase material i.e. AAFAM concrete under ambient and dry curing.

Table 3 Results of Alkali Activated Fly Ash Paste.

Molar Ratio Na₂O/SiO₂	Molar Ratio SiO₂/Al₂O₃	Molar Ratio H₂O/Na₂O	Molar Ratio H/NSA	Mass Ratio H/NSA	f_{c28} (MPa)	f_{c7} (MPa)
0.17	3.93	10.38	1.21	0.25	25.35	9.77
0.15	4.13	9.82	1.07	0.23	27.91	13.48
0.18	3.74	10.90	1.35	0.28	20.52	6.88
0.20	3.93	8.25	1.11	0.23	27.23	15.69
0.17	4.13	8.34	1.01	0.21	31.84	19.68
0.22	3.74	8.18	1.22	0.24	23.25	9.77
0.21	3.93	7.51	1.07	0.22	36.27	18.67
0.18	4.13	7.79	0.98	0.21	40.17	25.10
0.24	3.74	7.28	1.16	0.23	26.84	10.47
0.22	3.93	6.90	1.03	0.21	34.03	16.96
0.19	4.13	7.32	0.96	0.20	41.05	22.46
0.26	3.74	6.56	1.11	0.21	27.29	13.98

4.2 Verification by Secondary Data

The first verification was executed on the AAFAM concrete without superplasticizer, as described in the works of Songpiriyakij [14]. Songpiriyakij used two types of curing, i.e. ambient curing and dry curing at 60 °C in an oven for 24 h in order to make Mae Moh fly ash AAFAM concrete. Because Songpiriyakij gives no further information about the complete paste composition factor, the method described by Hardjito and Rangan [9] to calculate paste composition factors was applied to Songpiriyakij's work. The best relationship between compressive strength and paste composition factor is also built by the relationship of f_c versus molar ratio of H/NSA, as given in Figure 6. This works either under ambient curing or under dry curing.

The second verification was executed on the AAFAM concrete that used superplasticizer, as described in the works of the Geopolymer Concrete Research Group of Curtin University of Technology [9,15]. The collected samples were observed under dry curing 45-75 °C for 24-48 h. The best relationship between compressive strength and paste composition factor is also

built by the relationship between f_c versus molar ratio of H/NSA, as given in Figure 7. This works also for AAFAM concrete using superplasticizer under dry curing.

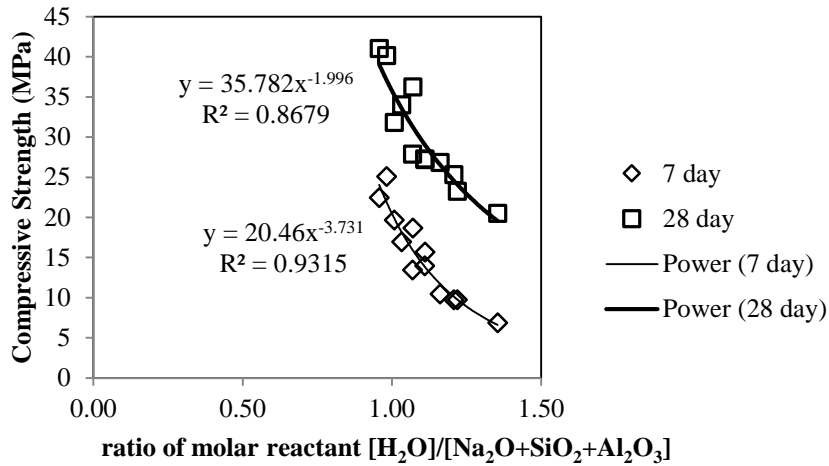


Figure 5 Relationships of compressive strength and molar ratio of H/NSA of AAFAM paste.

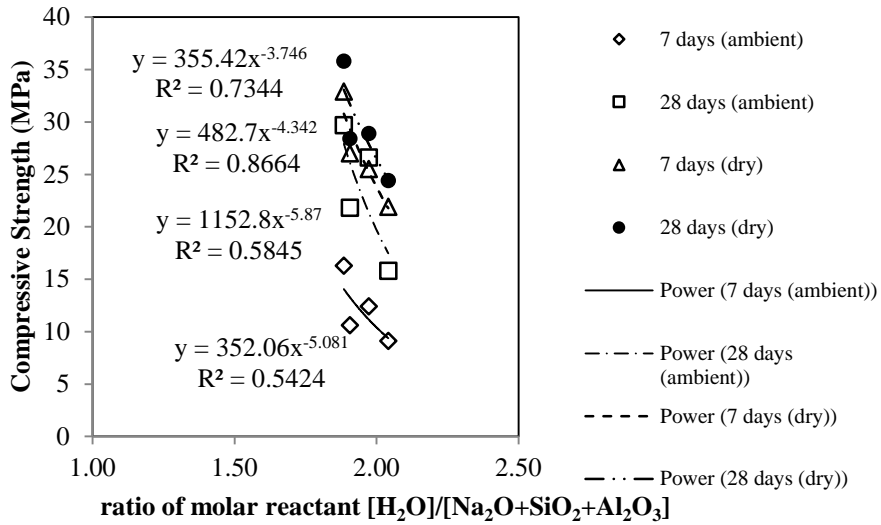


Figure 6 Relationships of compressive strength and ratio of molar reactant H/NSA analyzed based on Songpiriyakij's work [14].

Conforming to the results of the verification described before, it is proposed that the best relationship between compressive strength of AAFAM and paste composition is the function of f_c against molar ratio of $H_2O/(Na_2O+SiO_2+Al_2O_3)$ or molar ratio of H/NSA. This function is considered as a substitute of f_c versus w/c in OPC based materials.

Thus, a nomogram of AAFAM mortar can be constructed based on Monteiro-Helene’s nomogram, which will be presented in the next subsection.

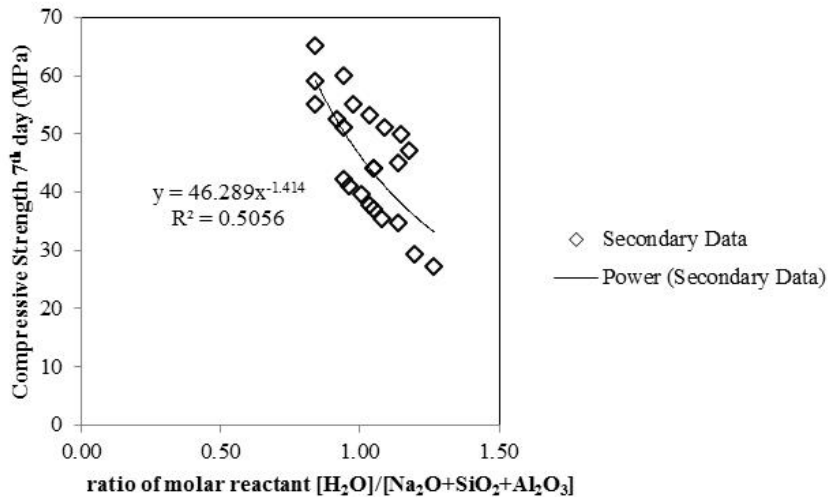


Figure 7 Relationships of compressive strength and molar ratio of H/NSA analyzed based on Hardjito-Rangan’s works [9] and Olivia-Nikraz’s works [15].

4.3 Nomogram of Mortar Phase

The characteristics of the AAFAM mortar mixtures as presented in Table 2 are given in Figure 8. Qualitatively, the flow test values are divided into three (3) categories describing the level of workability of the mortar: (1) <15 cm is categorized as low workability; (2) 15-20 cm is categorized as moderate workability; and (3) >20 cm is categorized as high workability.

This result also describes that the best relationship between the compressive strength of the material and the paste composition is the relationship of f_c versus molar ratio of H/NSA or f_c versus molar ratio of $H_2O/(Na_2O+SiO_2+Al_2O_3)$ with $R^2 = 0.7251$ using an exponential function. Meanwhile, workability according this relationship can be divided into the following categories: $R^2 = 0.6482$ for low workability, $R^2 = 0.3229$ for moderate workability and $R^2 = 0.8885$ for high workability.

To smoothen the graph and to simplify the discussion, the mixtures number 20 and 23 were excluded from the high workability mortars because they had almost the same compressive strength as others mixtures, i.e. (1) mixture 20 and mixture 18 had almost the same strength (55.75 MPa and 55.66 MPa), and (2) mixture 23 and mixture 19 had almost the same strength (47.98 MPa and 46.87 MPa). Then, the relationship of f_c versus H/NSA had $R^2 = 0.9696$ as shown in Figure 9.

The nomogram adapted from Monteiro-Helene's nomogram is shown in Figure 9. The modifications made are: (1) variable m , which represents the mass ratio of aggregate/cement in Monteiro-Helene's nomogram, was modified by using m' , which represents the mass ratio of the aggregate/paste, and (2) variable C , which represents the mass of cement per volume of mixture in Monteiro-Helene's nomogram, was modified using C' , which represents the mass of fly ash per m^3 of mixture.

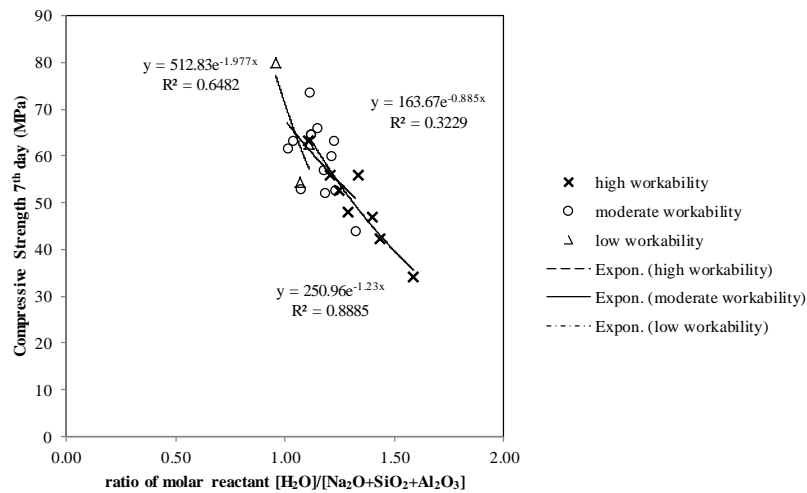


Figure 8 Relationships between compressive strength and molar ratio of H/NSA of AAFAM Mortar.

Figure 9 shows more scattered data in Lyse's and Molinary's modification graphs. This figure reveals that the compressive strengths of the mixtures that had a different fly ash content but the same aggregate content, were affected by the molar ratio of H/NSA. This result reveals that it is still possible to make a nomogram of AAFAM based on the nomogram of OPC.

4.4 Microscopic Characteristics of AAFAM Mortar

It is important to find out whether the solidification products or microscopic characteristics of the mortars that were used to build the nomogram were the same. This is to ascertain that the nomogram is only affected by macroscopic characteristics of the mortar. Therefore, 4 (four) representative mixtures of Table 2 were taken to be analyzed, i.e. mixture 3 (80 MPa); mixture 5 (53.3 MPa); mixture 20 (55.66 MPa); and mixture 24 (33.9 MPa).

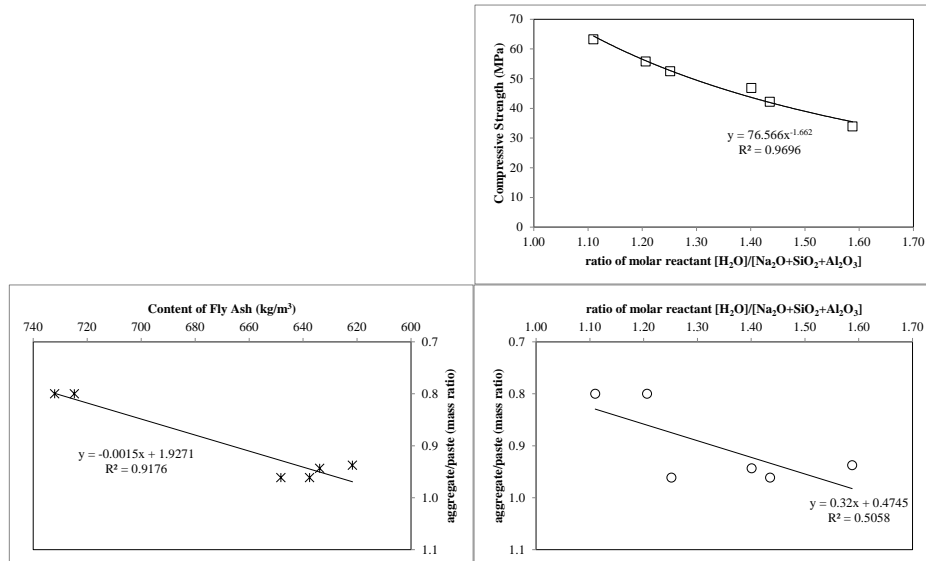


Figure 9 Relationships between compressive strength and molar ratio of H/NSA of high workability AAFAM mortar.

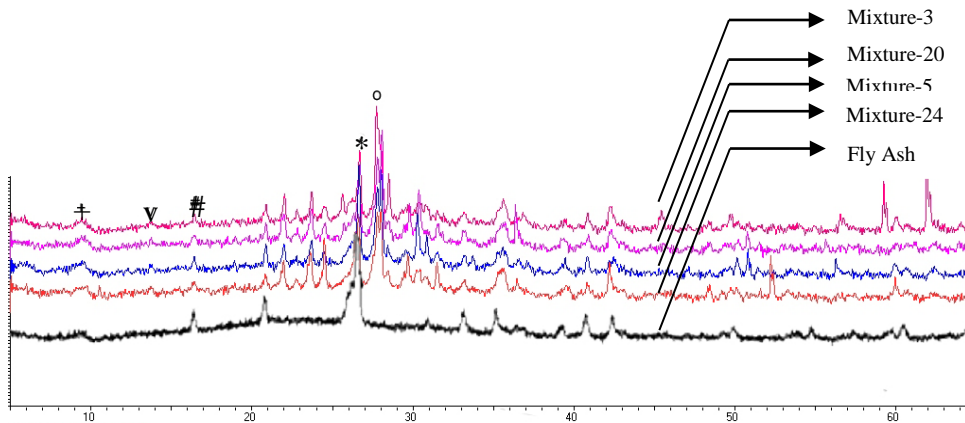


Figure 10 XRD Patterns of the AAFAM mortar { where : * = quartz (SiO_2), + = phyllopite ($\text{Al}_2\text{Si}_4\text{O}_{10}(\text{OH})_2$), # = mullite ($\text{Al}_6\text{Si}_2\text{O}_{13}$), o = albite ($\text{Na}(\text{Si}_3\text{Al})\text{O}_8$) and v = sodium aluminosilicate hydrate ($\text{Na}_6(\text{AlSiO}_4)_6 \cdot 4\text{H}_2\text{O}$) }.

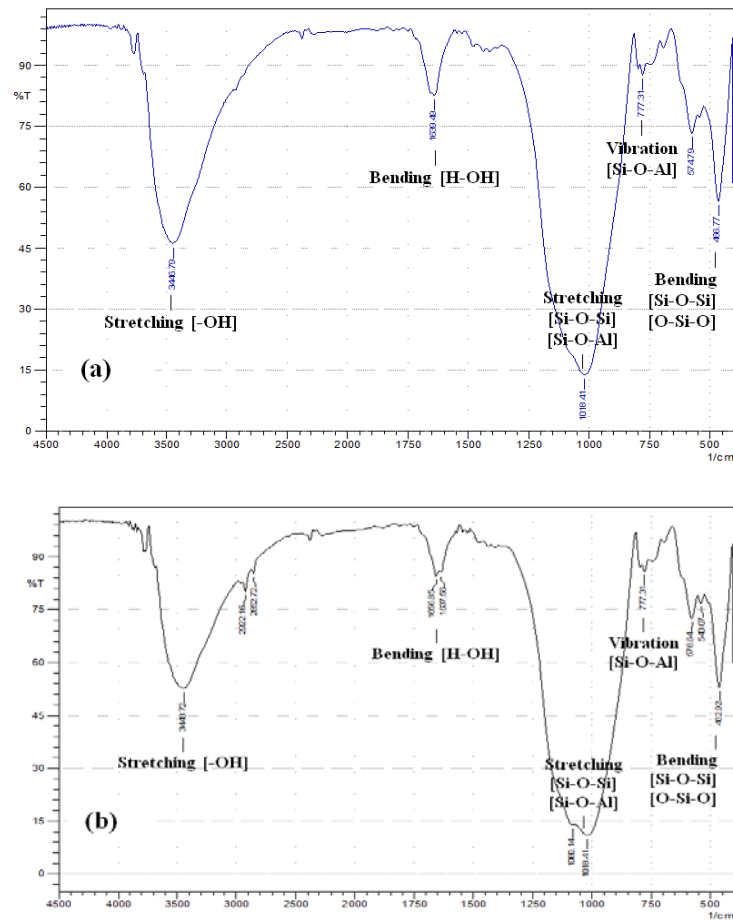


Figure 11 FTIR spectroscopy of AAFAM mortar: (a) Mixture 24 (33.9 MPa) and (b) Mixture 3 (80 MPa).

Table 4 Peaks of FTIR Spectroscopy.

Sample	Stretching -OH (cm ⁻¹)	Bending H-O-H (cm ⁻¹)	Stretching O-C-O (cm ⁻¹)	Stretching Si-O-Si Si-O-Al (cm ⁻¹)	Symmetric Vibration Si-O-Al (cm ⁻¹)	Bending Vibration Si-O-Si O-Si-O (cm ⁻¹)	
Fly Ash	2923.56	1627.63	-	1076.08	744.39	-	485.97
Mixture 24	3446.79	1639.49	-	1018.41	777.31	574.79	466.77
Mixture 20	3448.72	1639.49	-	1080.14;1010.17	777.31	574.79	462.92
Mixture 3	3448.72	1637.56	-	1080.14;1018.41	777.31	578.64	462.92
Mixture 5	3448.72	1641.42	1431.18	1024.20	777.31	572.86	462.92

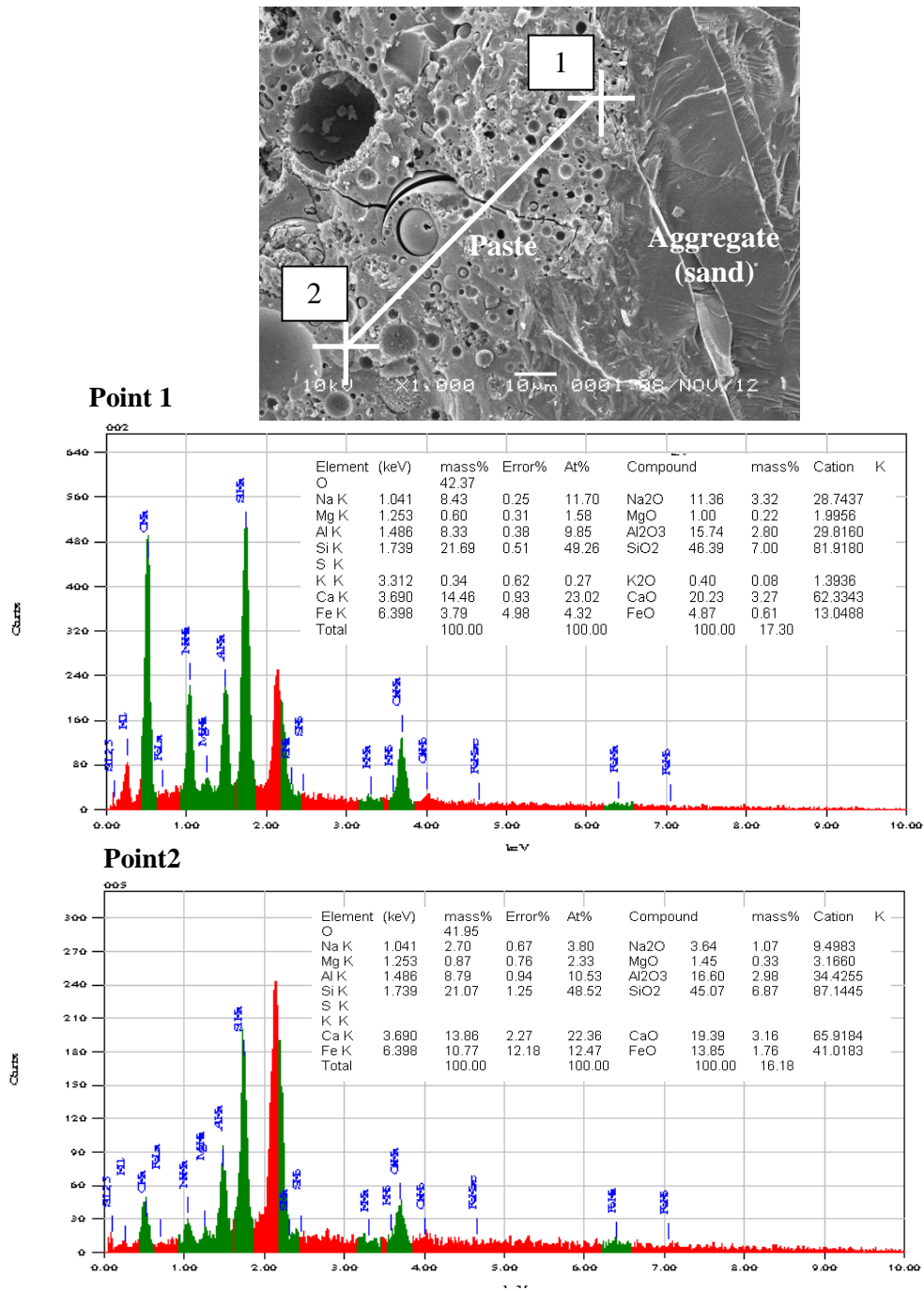
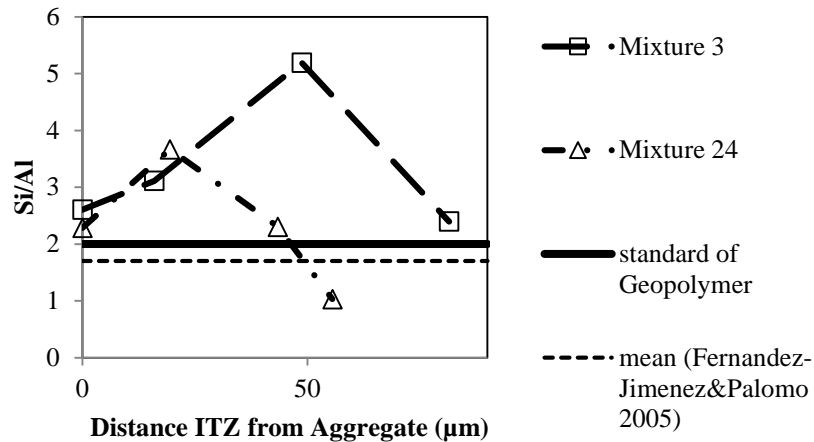
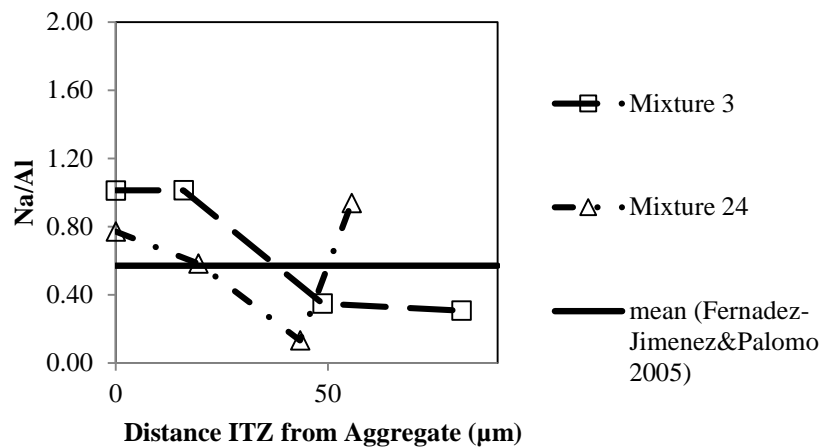


Figure 12 SEM+EDXA of AAFAM mortar on Mixture 3 (80 MPa).



(a)



(b)

Figure 13 Results of EDXA of Mixture 3 and Mixture 24: (a) ratio of Si/Al versus distance of ITZ, and (b) ratio of Na/Al versus distance of ITZ.

From the XRD spectroscopy in Figure 10 we can see that 2 (two) new minerals occurred compared to the fly ash as raw material, i.e. albite ($\text{Na}(\text{Si}_3\text{Al})\text{O}_8$) and sodium aluminosilicate hydrate ($\text{Na}_6(\text{AlSiO}_4)_6 \cdot 4\text{H}_2\text{O}$). These minerals were present in all mixtures. This indicates that sodium aluminosilicate gel forms were formed [16]. Therefore, the solid products of all mortars were the same. Meanwhile, the quartz and mullite from the fly ash had not been altered. This is the same result as in Fernandez-Jimenez, *et al.* [16] and Skavara, *et al.* [17].

Meanwhile from the FTIR spectroscopy in Figure 11 or its resume in Table 4 it can be seen that the stretching vibration peaks of Si-O-Si or Si-O-Al in the AAFAM mortars (1018.41, 1010.17, 1018.41, 1024.2 cm^{-1}) were lower compared to those in the peak of fly ash (1076.08 cm^{-1}). This is an indication that sodium alumina silicate hydrate was formed [16]. Mixture 3 and mixture 20 had 2 (two) peaks, indicating stretching vibration of Si-O-Si or Si-O-Al, even at a higher wavelength number at 1080.14 cm^{-1} . Probably, this is the effect of 'pendular movement' that evolved into a Si-rich gel increasing the mechanical properties of the material [18]. In mixture 5, a trona or sodium bicarbonate band at 1431.18 cm^{-1} has been indicated. Fernandez-Jimenez, *et al.* [16] also found this indication when using NaOH+Na₂CO₃ as activator. However, in mixture 5, trona probably occurred because of the presence of CO₂ in the air.

Then, by using SEM-EDXA in line through the interfacial transition zone (given in Figure 12), it was indicated that the ratios of Si/Al and Na/Al of mixture 3 were higher than those of mixture 24 (given in Figure 13(a) and 13(b)). According to the SEM-EDXA results there was no ITZ in any of the mixtures. All mortars had a similar morphology.

5 Conclusions

It is proposed that the relationship of f_c versus molar ratio of $\text{H}_2\text{O}/(\text{Na}_2\text{O}+\text{SiO}_2+\text{Al}_2\text{O}_3)$ or molar ratio of H/NSA in AAFAM can substitute the relationship of f_c versus water/cement (w/c) in OPC based materials. That relationship works well in every phase of AAFAM, i.e. paste, mortar and concrete, either under ambient or dry curing and with or without superplasticizer.

This paper also presents the development of a nomogram for AAFAM mixtures in mortar phase. It is possible to construct a nomogram for AAFAM mortar based on the nomogram of OPC based materials. In this study, Monteiro-Helene's nomogram was used as the framework for the development of the AAFAM nomogram.

The AAFAM mortars in the nomogram have similar solidification products based on the XRD, FTIR and SEM-EDXA analyses. This means that the nomogram is only affected by macroscopic characteristics of the mortar.

Acknowledgements

The research presented in this paper was funded by the Directorate General of Higher Education Indonesia (Dikti) through a National Strategic Competitive Research Grant 2010-2011. The financial support received is gratefully

acknowledged. The authors would also like to thank Andrie Harmaji for helping in the AAFAM mortar research.

Nomenclature

m	=	Mass ratio of aggregate/cement (kg/kg) for OPC based materials
C	=	Cement content per volume of mixture (kg/m ³) for OPC based materials
f_c	=	Compressive strength at rupture
m'	=	Mass ratio of aggregate/paste (kg/kg) for AAFAM mortar
C'	=	Fly ash content per volume of mixture ((kg/m ³) for AAFAM mortar
H/NSA	=	Molar ratio of H ₂ O/(Na ₂ O+SiO ₂ +Al ₂ O ₃) of AAFAM paste

References

- [1] Davidovits, J., *Geopolymer: Chemistry and Applications*, 2nd ed., Institut Geopolymer, 2008.
- [2] Pacheco-Torgal, F., Castro-Gomes, J. & Jalali, S., *Alkali Activated Binders: A review, Part 1, Historical Background, Terminology, Reaction Mechanisms and Hydration Products*, Construction and Building Materials, **22**, pp. 1305-1314, 2008.
- [3] Duxson, P., Fernandez-Jimenez, A., Provis, J.L., Lukey, G.C., Palomo, A. & van Deventer J.S.J., *Geopolymer Technology: The Current State of the Art*, Material Science, **42**, pp. 2917-2933, 2007.
- [4] Fernandez-Jimenez, A., Garcia-Lodeiro, I. & Palomo, A., *Durability of Alkali-Activated Fly Ash Cementitious Materials*, Material Science, **42**, pp. 3055-3065, 2007.
- [5] Temuujin, J., Minjingmaa, A., Lee, M., Chen-Tan, N. & van Rissen, A., *Characterisation of Class F Fly Ash Geopolymer Pastes immersed in Acid and Alkaline Solution*, Cement and Concrete Composites, **33**, pp. 1086-1091, 2011.
- [6] Pacheco-Torgal, F., Castro-Gomes, J. & Jalali, S., *Alkali Activated Binders: A review Part 2, About Materials and Binders Manufacture*, Construction and Building Materials, **22**, pp. 1315-1322, 2008.
- [7] Van Deventer, J.S.J., Provis, J.L. & Duxson, P., *Technical and Commercial Progress in The Adoption of Geopolymer Cement*, Minerals Engineering, **29**, pp. 89-104, 2012.
- [8] Monteiro, P.J.M. & Helene, P.R.L., *Designing Concrete Mixtures for Desired Mechanical Properties and Durability*, in Proceedings of V.Mohan Malhotra Symposium on Concrete Technology: Present and Future, SP-144, ACI, Detroit-USA, P Kumar Mehta (ed.), pp. 519-543, 1994.

- [9] Hardjito, D. & Rangan, B.V., *Development and Properties of Low-Calcium Fly Ash-Based Geopolymer Concrete*, Research Report GC1, Faculty Engineering, Curtin University of Technology, Perth, Australia, 2005.
- [10] Anuradha, R., Sreevidya, V., Venkatasubramani, R. & Rangan, B.V., *Modified Guidelines for Geopolymer Concrete Mix Design Using Indian Standard*, Asian Journal of Civil Engineering (Building and Housing), **13**(3), pp. 353-364, 2012.
- [11] Simatupang, P.H., Imran, I., Pane, I. & Sunendar, B., *The Comparison of Microscopic and Macroscopic Characteristics Between Low Calcium Fly Ash Geopolymer Binder and High Calcium Fly Ash Geopolymer Binder Using Indonesian Fly Ash*, in Proceedings of the 3rd International Conference of European Asian Civil Engineering Forum (EACEF), Yogyakarta-Indonesia, Anastasia Yunika & Ferianto Raharjo (eds), pp. B27-B32, 2011.
- [12] Simatupang, P.H., Imran, I. & Pane, I., *The Latest Development of Green Concrete in Indonesia*, in Proceedings of the 1st International Conference on Sustainable Civil Engineering Structures and Construction Materials (SCESCM), Yogyakarta-Indonesia, Priyosulistyo, Suhendro B., Kanie S., Satyarno I., Senjutichai T., Triwiyono A., Sulistyo D., Siswosukarto S. and Awaludin A. (eds), pp. 62-69, 2012.
- [13] Pacheco-Torgal, F., Abdollahnejad, Z., Camoes, A.F., Jamshidi, M. & Ding, Y., *Durability of Alkali Activated Binders: A Clear Advantage over Portland Cement or an Unproven Issue?*, Construction and Building Materials, **30**, pp. 400-405, 2012.
- [14] Songpiriyakij, S., *Engineering Properties of Mae Moh Fly Ash Geopolymer Concrete*, International Conference on Pozzolan, Concrete and Geopolymer, KhonKaen, Thailand, 24-25 May, 219-225, 2006, <http://www.smith-kmitab.com/publication/pcg31.pdf> (1 March 2013).
- [15] Olivia, M. & Nikraz, H., *Properties of Fly Ash Geopolymer Concrete Designed by Taguchi Method*, Materials and Design, **36**, pp. 191-198, 2012.
- [16] Fernandez-Jimenez, A. & Palomo, A., *Composition and Microstructure of Alkali Activated Fly Ash Binder: Effect of Activator*, Cement and Concrete Research, **35**, pp. 1984-1992, 2005.
- [17] Skvara, F., Jilek, T. & Kopecky, L., *Geopolymer Materials Based on Fly Ash*, Ceramics-Silikaty, **49**(3), pp. 195-204, 2005.
- [18] Criado, M., Fernandez-Jimenez, A. & Palomo, A., *Alkali Activation of Fly Ash, Effect of the SiO₂/Na₂O ratio. Part I. FTIR Study*, Micropor Mesopor Material, **106**, pp. 180-191, 2007.